Primljeno / Received: 29.09.2025.
Ispravljeno / Corrected: 08.11.2025
Prihvaćeno / Accepted: 20.11.2025.

UDK 528.2(497.7)
Pregledni naučni rad / Review article
DOI: https://doi.org/10.58817/2233-1786.2025.59.56.97

VALIDATION OF SATELLITE-ONLY GGMS OVER THE WESTERN PART OF NORTH MACEDONIA

VALIDACIJA SATELITSKIH GGMS NAD TERITORIJOM ZAPADNOG DIJELA SJEVERNE MAKEDONIJE

Filip Petrovski

ABSTRACT

The purpose of this research is to identify the most suitable Global Geopotential Model (GGM) for geoid determination in a specific region of Western Macedonia. The selection of the most suitable GGM eliminates the evaluation of numerous alternatives and provides a reliable reference for future geoid model enhancement. Some validation methods were applied, including the comparison of geoid undulations, free-air gravity anomalies, and Bouguer anomalies. The results highlight variations in performance among the tested GGMs and indicate the model best suited for subsequent research. The adoption of a tested GGM for geoid determination will significantly reduce the reliance on labor-intensive spirit leveling and allow for the effective use of GNSS observations in determining orthometric heights, particularly in mountainous terrain.

Keywords: global geopotential model, gravity anomalies, geoid undulation, GNSS/levelling, CSH

SAŽETAK

Cilj ovog istraživanja je identifikacija najprikladnijeg Globalnog geopotencijalnog modela (GGM) za određivanje geoida na području zapadne Makedonije. Odabir optimalnog GGM-a uklanja potrebu za razmatranjem brojnih alternativnih rješenja i predstavlja pouzdanu osnovu za buduće unapređenje geoidnog modela. U istraživanju su primijenjene različite metode validacije, uključujući poređenje geoidnih undulacija, anomalija slobodnog vazduha i Bugeovih anomalija. Dobijeni rezultati ukazuju na varijacije u performansama među analiziranim GGM-ovima i omogućavaju identifikaciju modela najprikladnijeg za dalja istraživanja. Usvajanjem testiranog GGM-a za određivanje geoida, značajno će se smanjiti oslanjanje na zahtjevno geometriskog nivelisanje i omogućiti efikasna upotreba GNSS opservacija u određivanju ortometrijskih visina, posebno u planinskim područjima.

Ključne riječi: globalni geopotencijalni model, gravitacijske anomalije, geoidne undulacija, GNSS/nivelman, CSH

Citiranje članka / To cite this article: Petrovski, F. (2025). Validation of Satellite-Only GGMs over the Western Part of North Macedonia. *Geodetski glasnik, 56*, 97-112. | https://doi.org/10.58817/2233-1786.2025.59.56.97

1 INTRODUCTION

Global Geopotential Models (GGMs) serve as fundamental data sources for modeling the long-wavelength components of the Earth's gravity potential (Varga, 2018). GGMs represent comprehensive models of the geopotential, from which various gravity-related quantities, such as geoid undulations, gravity anomalies, height anomalies, and deflections of the vertical, can be derived. These models are particularly useful for representing the long-wavelength spatial features of the gravity field. GGMs are generally classified into three types based on the data used for their development: satellite-only, combined, and tailored (Vaníček and Featherstone, 1998; Abbak et al., 2012).

The development of GGMs dates back to the 1960s with early satellite missions, but substantial progress occurred in the 21st century with missions such as CHAMP (CHallenging Mini-satellite Payload for geophysical research and application), GRACE (Gravity Recovery and Climate Experiment), and GOCE (Gravity field and steady-state Ocean Circulation Explorer). These missions facilitated the collection and processing of extensive datasets, resulting in the publication of over 180 GGMs currently available via the International Centre for Global Earth Models (ICGEM) (Ince et al., 2019). For this study, satellite-only gravity field models derived from the GRACE and GOCE missions are utilized, as they represent the most recently developed and refined models available.

Several similar studies have been conducted: assessment of GOCE derived models over are in Turkey with different maximum degree of expansion which yielded 15 % improvement in gravimetric geoid determination (Erol et al., 2020), combined GGMs were evaluated over Vietnam with XGM2019e_2159 model fitting the best on the GNSS/levelling data (Pham et al., 2023), validation of GGMs using gravity anomalies in Poland (Godah et al., 2018), some recent GGMs were evaluted spectrally and regionally in Türkiye (Ustun and Abbak, 2010), combined GGMs assessed over Kenya on 55 GNSS/levelling points with SGG-UGM-1 and SGG-UGM-2 yielding best fit (Nyoka et al., 2022), and validation over Kuwait with GO_CONS_GCF_2_SPW_R5 resulting in smallest standard deviation (El-Ashquer et al., 2020).

The study begins with a detailed description of the research area, including its topographic characteristics. Thereafter, the datasets necessary for the assessment of GGMs are outlined. These include GNSS/leveling observations, and gravity measurements, in addition to the GGMs themselves. Comparisons are conducted against geometric geoid undulations and gravity anomalies. Finally, all GGMs are evaluated with the mean and the standard deviation of the differences in the geoid undulations with varying maximum degree of expansion. Numerical results show that GOCE based GGMs have good agreement with terrestrial data in our study area.

This study represents the first comprehensive investigation of its kind conducted within the Republic of North Macedonia, integrating multiple types of geospatial and geophysical datasets. The use of data in this study is restricted to a specific region of the country due to data access limitations imposed by the Agency for Real Estate Cadastre of North Macedonia (AREC), which granted permission for use only within the designated area. To the author knowledge, no previous research has combined these diverse data sources for this region, making this work a significant contribution toward improving the understanding of its geodetic and geophysical characteristics.

2 DATA AND METHODOLOGY

In this study, several methods are employed to evaluate the performance of the GGMs. This chapter presents the methodologies and datasets used in the analysis. The methodologies for evaluation include comparisons between the geoid undulations and gravity anomalies derived from the GGMs and those obtained from terrestrial measurements. Additionally, geoid undulation differences are analyzed with respect to varying maximum degrees of spherical harmonic expansion for the GGMs considered.

2.1 Study area

For the present study, a specific region in the western part of the Republic of Macedonia was selected. This area exhibits complex topography, with orthometric heights ranging from approximately 600 to 2100 meters. The datasets utilized in the analysis were obtained from multiple sources: GGMs, which are publicly accessible, as well as GNSS/leveling observations, and gravity data provided by AREC (AREC, 2025). This region is defined by the $\varphi_{\min} = 41°18'18'', \varphi_{\max} = 41°38'42'', \lambda_{\min} = 20°39'18'', \lambda_{\max} = 20°59'42''$. A detailed description of the data utilized in this study is provided in the following subsections.

2.2 Global geopotential models

In geodesy, the mathematical function that approximates the real gravitational potential in the free space outside the Earth is referred to as the global gravity field model or GGM. From such a model, purely gravitational quantities, such as the magnitude and vector of the Earth's gravity as well as the gravitational potential, can be computed. However, quantities such as geoid undulations, gravity anomalies, and the disturbing potential can only be determined with respect to a selected reference ellipsoid (Moritz, 1980). The centrifugal potential is an analytical function, which leaves the computation of the gravitational potential as a harmonic function in the free space outside the Earth. The representation of the gravitational potential is carried out using spherical harmonic functions, which satisfy Laplace's equation (Heiskanen & Moritz, 1967). Accordingly, the Earth's gravitational potential V, both on and above its surface, can be expressed as a summation of spherical harmonics of a given degree and order. Beside the gravitational potential, we can express the disturbing potential as a series of spherical harmonics, which results in obtaining the data needed for calculation of the geoid undulation, using Eq. (1) known as Bruns formula (Bruns, 1878):

$$N = \frac{T}{\gamma}, \tag{1}$$

where T is the disturbing potential, γ is normal gravity on level-ellipsoid. Over the past two decades, GGMs have significantly improved in quality and are now widely applied in numerous geodetic and geophysical studies. Consequently, a validation procedure is required to assess the accuracy with which these models represent the Earth's geopotential (Yilmaz & Cakir, 2025). The outcomes of such validation are particularly important for geoid determination, as they provide the basis for identifying the most suitable GGM for a specific study area, selecting the optimal maximum degree of expansion, and conducting quality assessments, cross-checks, and the detection of outliers and systematic errors in gravity or GNSS/levelling datasets. Two functionals of the gravity field potential: geoid undulation N_{GGM} and free-air gravity anomaly Δg_{GGM} are derived from the spherical harmonic coefficients of each GGM using equations (2) and (3) (Hofmann-Wellenhof and Mortiz, 2006):

$$N_{GGM} = \frac{GM}{\gamma r} \sum_{n=2}^{n_{\max}} \left(\frac{a}{r}\right)^{n} \sum_{m=0}^{n} x(\Delta\bar{C}_{nm}\cos m\lambda + \bar{S}_{nm}\sin m\lambda)\bar{P}_{nm}(\cos\theta), \tag{2}$$

and

$$\Delta g_{GGM} = \frac{GM}{r^2} \sum_{n=2}^{n_{\max}} (n-1) \left(\frac{a}{r}\right)^{n} \sum_{m=0}^{n} x(\Delta\bar{C}_{nm}\cos m\lambda + \bar{S}_{\mathrm{nm}}\sin m\lambda)\bar{P}_{nm}(\cos\theta). \tag{3}$$

where *GM* presents the product of the Earth's mass and the Newtonian gravitational constant, *r* refers to the radial distance of the computation point, $n_{\max}$ is the maximum degree of expansion, *n* is the degree and *m* is the order of the selected GGM, *a* indicates the semi-major axis of the level-ellipsoid, $\bar{C}_{nm}$ and $\bar{S}_{nm}$ are fully normalized coefficients, Δ is the coefficients' differences between GGM and level-ellipsoid, and $\bar{P}_{nm}$ refers the first kind of fully normalized Legendre function. The GGMs selected for validation are shown in Table 1.

Table 1.
Selected GGMs for validation

Model name	Year published	n_{max}	Mission	Source
HUST-Grace2016s	2016	160	GRACE	(Zhou et al., 2017)
ITU_GGC16	2016	280	GRACE+GOCE	(Akyilmaz et al., 2016)
Tongji-Grace02k	2018	180	GRACE	(Q. Chen et al., 2018)
GOSG01S	2018	220	GOCE	(Xinyu Xu et al., 2017)
GO_CONS_GCF_2_TIM_R6	2019	300	GOCE	(Brockmann et al., 2019)
Tongji-GMMG2021S	2022	300	GRACE+GOCE	(J. Chen et al., 2022)
GOSG02S	2023	300	GOCE	(Xinyu; Xu et al., 2023)
WHU-SWPU-GOGR2022S	2023	300	GRACE+GOCE	(Zhao et al., 2023)

2.3 Gravity data

Another validation method for the GGMs is using the terrestrial gravity data tested against the data obtained from the GGM using Eq. (3). Gravity data in Republic of Macedonia are gathered during the campaign carried out from 2010 until 2014 when a new gravimetric network was established. For this study, a total of 165 gravity measurement points were provided by AREC, exhibiting a relatively uniform spatial distribution of approximately one point per 6 km², as illustrated in Figure 1. The instruments employed are relative gravimeters SCINTREX – CG5 and SCINTREX CG3+. Positional coordinates are given in the European Terrestrial Reference System 1989 (ETRS89) and refers to the GRS80 ellipsoid. The accuracy of the data is shown in Table 2. These data were utilized to compute the free-air and simple Bouguer gravity anomalies, whereas the GGM anomalies were obtained from the ICGEM (Ince et al., 2019).

Table 2.
Gravity network data in Republic of Macedonia (Kasapovski *et al.*, 2018)

Rank	Zero	First	Second
Year of measurement	2010	2013	2014
Number of points	3	25	2310
Accuracy	3 μgal	13 μgal	< 60 μgal

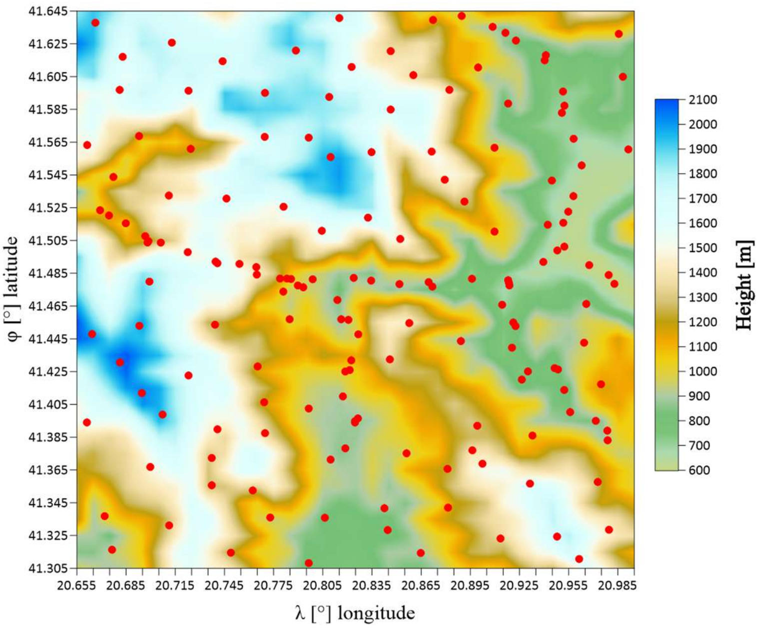

Figure 1. Distribution of gravity data.

Gravity anomalies represent a fundamental dataset in geoid modelling. They are defined as the difference between gravity measurements, and the corresponding normal gravity values on a reference ellipsoid (Heiskanen & Moritz, 1967). Such anomalies reflect deviations between the geoid and the reference ellipsoid, heterogeneities in the subsurface mass distribution, and, in some cases, residual measurement errors.

Although various types of gravity anomalies are recognized in physical geodesy, the present study is restricted to free-air and simple Bouguer anomalies, which serve as the primary basis for the subsequent GGMs evaluation.

The free-air anomalies are calculated using Eq. (4):

$$\Delta g_{FA} = g + \delta_{FA} - \gamma, \tag{4}$$

and the simple Bouguer anomalies are calculated using Eq. (5):

$$\Delta g_{SB} = g + \delta_{FA} + \delta_{SB} - \gamma, \tag{5}$$

where Δg_{FA} is the free-air anomaly, g is gravity, δ_{FA} is the free-air reduction, δ_{SB} is the simple Bouguer reduction, Δg_{SB} is the simple Bouguer anomaly, and γ is the normal gravity on the reference ellipsoid.

Bouguer reductions are categorized as either simple or complete, with the simple Bouguer reduction having a magnitude equal to, but opposite in sign from, the gravitational attraction exerted by the equivalent slab. For these two quantities, the following Eq. (6) and Eq. (7) are used:

$$\delta_{FA} = 0.3086 * H, \tag{6}$$

and

$$\delta_{SB} = -2\pi G\rho H. \tag{7}$$

If we use the values for $G = 6.67 \times 10^{-11}\ \frac{\mathrm{m}^3}{\mathrm{kg}^{\ 2}}$ and $\rho = 2670\ \frac{kg}{m^3}$, then we obtain the Bouguer reduction calculated using Eq. (8):

$$\delta_{SB} = -0.1119 * H. \tag{8}$$

For these equations, we implement the orthometric height in meters, while the results of the calculations are expressed as miligals [mGal]. This unit is furthermore employed throughout the following analyses.

2.4 GNSS/levelling data

The fundamental leveling network constitutes a component of the national geodetic infrastructure and serves as the vertical reference framework for all height surveys conducted in the Republic of Macedonia. It also provides the basis for the realization of significant scientific, engineering, and technical tasks. The network is organized into several classes, among which the first- and second-order networks represent the highest accuracy. These high-precision surveys are employed in scientific investigations related to the determination of the Earth's figure, monitoring vertical crustal movements, and assessing differences in sea and ocean levels. The newly established high-accuracy leveling network (NVT3) comprises 1,098 leveling benchmarks interconnected by 49 leveling lines and 19 polygons, supplemented by 12 connection lines to neighboring countries. The total length of the leveling traverses amounts to 2,189 km, with an average spacing of approximately 1,800 m between benchmarks and an average polygon perimeter of 166 km. The network further includes 28 fundamental benchmarks and 31 nodal points (Odalovic, 2009). For the accuracy determination of the GGMs, 46 GNSS/levelling points are used as illustrated in Figure. The accuracy of the GNSS points is 4 mm horizontally and 6 mm vertically as provided by AREC. The accuracy of the levelled height differences in NVT3 is approximately 0.3 mm.

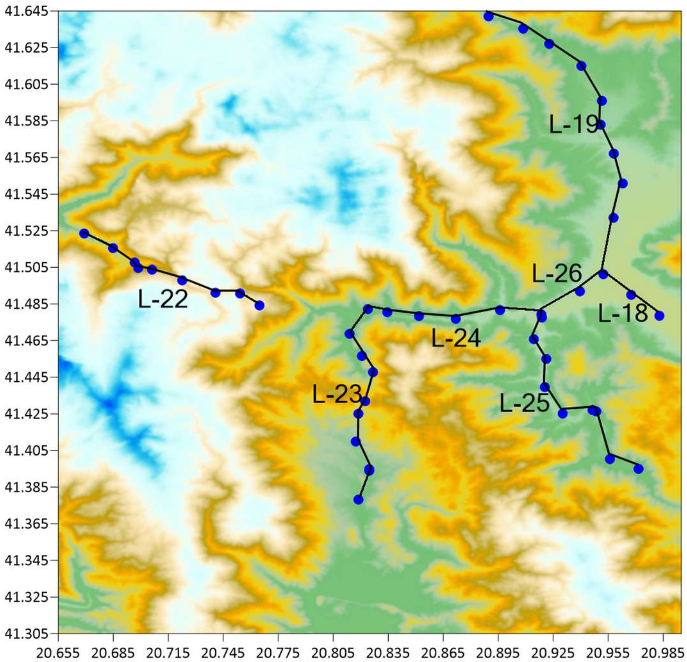

Figure 2. Distribution of GNSS/levelling data.

2.5 Validation methodology

The selection of the GGMs for validation is done by the year of publishing (not older than 10 years) and satellite-only (GOCE, GRACE, GOCE+GRACE). The validation is done in several steps (Varga, 2018):

- Statistical analysis of δN using maximum degree of the model

The initial assessment of the GGMs is performed through comparison with ground-based GNSS/leveling data. In this approach, the geometric geoid undulations are derived by combining the ellipsoidal height (h), obtained from GNSS observations, with the orthometric height (H), determined from spirit leveling. The geometric undulation (N) is then computed as the difference between these two height systems. with Eq. (9):

$$N_{GNSS-level.} = h - H. \tag{9}$$

By using the values obtained with Eq. (2) and Eq. (9) in Eq. (10), we can calculate the differences:

$$\delta N = N_{GNSS-level.} - N_{GGM}. \tag{10}$$

- Statistical analysis of $\delta \Delta g$ using maximum degree of the model

The second assessment was carried out on the gravity observation points by calculating the differences between the terrestrial free-air gravity anomalies and the corresponding free-air anomalies derived from the GGM. These calculations were performed using Eq. (11):

$$\delta g_{FA} = \Delta g_{FA} - \Delta g_{GGM}. \quad (11)$$

As explained before, Δg_{FA} is calculated using Eq. (4), and Δg_{GGM} by using Eq. (3).

- Graphical analysis of the differences as a function of different variables (latitude, longitude, geoid undulation, orthometric height, free-air anomalies, Bouguer anomalies);
- Graphical analysis of the mean and standard deviation of δN using different maximum degree of expansion for the GGMs.

3 RESULTS

Validation of GGMs is a crucial step in evaluating their accuracy and reliability in representing the Earth's geopotential field. In this study, three types of validation are performed: validation using GNSS/levelling data, validation using gravity data, and validation based on the variation of the maximum degree of spherical harmonic expansion of the GGMs.

For the validations based on GNSS/levelling and gravity data, the maximum degree of expansion is employed for each GGM to compute the corresponding geoid undulations and free-air gravity anomalies. In the third type of validation, gravimetric geoid undulations corresponding to different maximum degrees of expansion are obtained from the ICGEM user service for the analysis (GFZ, 2025).

3.1 Validation of GGM by means of GNSS/levelling data

The calculated differences using Eq. (10) can be used for determination of the minimum, maximum, mean and root mean square error *(RMS)*. The statistics of the comparison is shown in Table 3.

Table 3.
Statistics of geoid undulation differences, units: [cm]

Model name	Min.	Max.	Mean	RMS
Tongji-Grace02k	-105.48	2.92	-38.88	30.06
HUST-Grace2016s	-174.38	-82.78	-118.05	25.22
GOSG02S	-39.88	39.61	10.88	21.20
GO_CONS_GCF_2_TIM_R6	-41.38	41.02	11	22.08
GOSG01S	-62.48	15.88	-11.62	21.60
WHU-SWPU-GOGR2022S	-40.68	38.71	10.02	21.21
Tongji-GMMG2021S	-48.18	32.01	2.88	21.30
ITU_GGC16	-59.48	23.82	-6.57	22.21

From the comparison, it can be concluded that almost all of the GGMs resulted in similar RMS, except for Tongji-Grace02k (30.06 cm) and HUST-Grace2016s (25.22 cm). Both of these GGMs are GRACE-only. The model which resulted in smallest RMS is GOSG02S which is GOCE-only GGM, but the others models yielded a similar error with discrepancies ranging up to 1.1 cm (ITU_GGC16). The model GOSG02S is chosen for the following figures, where the differences are a function of variables. From Figure we can see that the differences are ranging from -20 cm to 10 cm for approximate orthometric height from 600 m to 1000 m. For heights above 1000 m, the differences starts to have larger values from 30 cm to 65 cm. On the right, we can see that the differences are not so dependable on the values of the geoid undulations, since for undulation value from 43.5 m to 44 m, the differences range from -20 cm up to 64 cm.

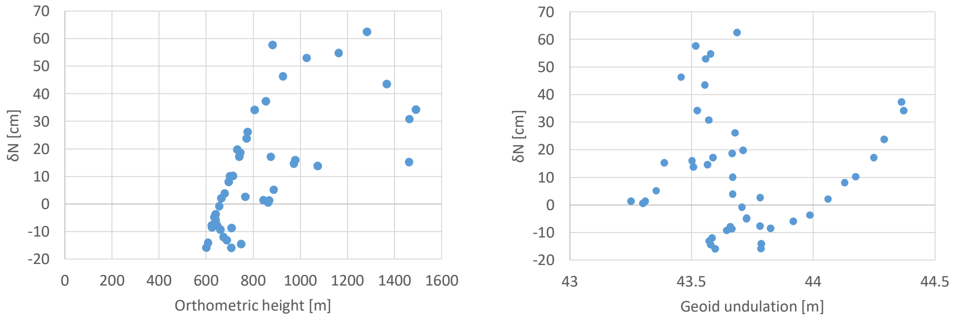

Figure 3. Geoid undulation differences as a function of orthometric height (left) and geoid undulation (right).

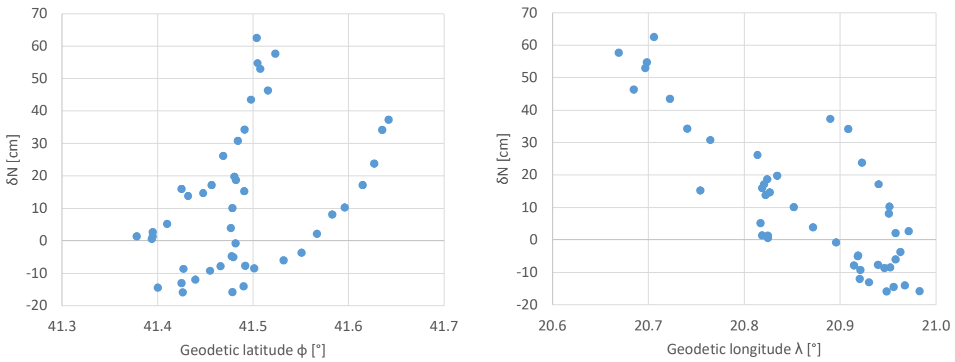

Figure 4. Geoid undulation differences as a function of latitude (left) and longitude (right).

Figure (left) presents the analysis of the differences as a function of latitude. It is noteworthy that the pattern of the differences closely resembles that shown in Figure (right), where the differences are analyzed as a function of geoid undulation. Furthermore, as previously noted, the differences do not exhibit a specific trend. For instance, at a latitude of approximately 41.5°, the values range from −20 cm to 65 cm. In contrast, the analysis of δN as a function of longitude (Figure , right) reveals a clear trend of decreasing differences toward the east (20.9°–21.0°). Larger differences, ranging from 40 cm to 63 cm, are observed around 20.7° longitude, which corresponds to mountainous terrain with elevations of approximately 1900–2000 m.

Figure illustrates the differences as a function of various types of gravity anomalies. The results indicate that larger anomaly values correspond to larger differences. On the left of Figure, for anomaly values between 90 and 120 mGal, the δN ranges from -20 cm to 10 cm, while for anomaly values exceeding 120 mGal, δN increases to a range from 20 cm to 65 cm. On the right of Figure, for values of Δg_{SB} around 30 mGal, δN varies between -15 cm and 10 cm. Beyond this, δN increases more rapidly, reaching values between 20 cm and 60 cm for Δg_{SB} values in the range of 60 mGal to 150 mGal. In comparison, both trends exhibit similar behavior, reflecting the dependence of gravity anomalies on height.

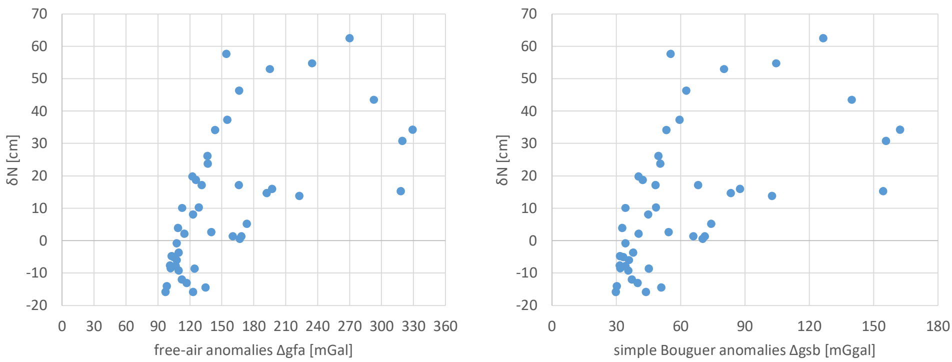

Figure 5. Geoid undulation differences as a function of free-air anomalies (left) and simple Bouguer anomalies (right).

3.2 Validation of GGMs on gravity points

The results from Eq. (11) are used for determination of the minimum, maximum, mean and RMS. The statistics of the comparison is tabulated in Table 4.

Table 4.
Statistics of gravity anomalies differences, units: [mGal]

Model name	Min.	Max.	Mean	RMS
Tongji-Grace02k	-73.57	108.12	4.78	45.65
HUST-Grace2016s	-51.48	126.59	25.06	51.09
GOSG02S	-89.04	85.8	-14.44	46.03
GO_CONS_GCF_2_TIM_R6	-90.25	86.03	-15.04	46.40
GOSG01S	-76.98	91.58	-5.11	44.65
WHU-SWPU-GOGR2022S	-89.06	85.79	-14.46	46.03
Tongji-GMMG2021S	-86.46	87.09	-12.21	45.54
ITU_GGC16	-81.66	93.64	-6.99	44.64

The comparison indicates that nearly all of the GGMs yielded similar RMS values, with the exception of HUST-Grace2016s, which exhibited an RMS of 51.09 mGal. The models producing the smallest RMS values are GOSG01S (GOCE) and ITU_GGC16 (GOCE+GRACE). The differences in RMS among the models range from 0.90 mGal to 1.76 mGal. For the subsequent figures, the GOSG01S model is selected, where the differences are analyzed as a function of the relevant variables.

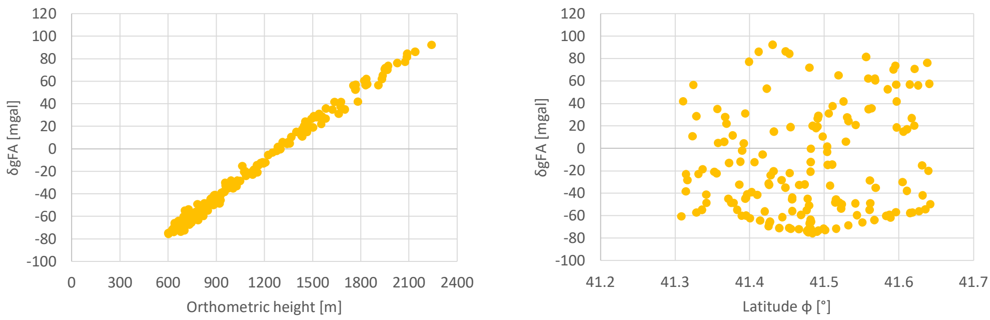

Figure 6. Gravity anomalies differences as a function of orthometric height (left) and latitude (right).

Figure presents the analysis of the differences as a function of orthometric height (left) and latitude (right). As expected, the differences increase with elevation. For heights between 600 m and 2000 m, the values range from −80 mGal to 80 mGal. In contrast, no significant trend is observed with latitude, as for any given latitude the differences vary within the same range from −80 mGal to 80 mGal.

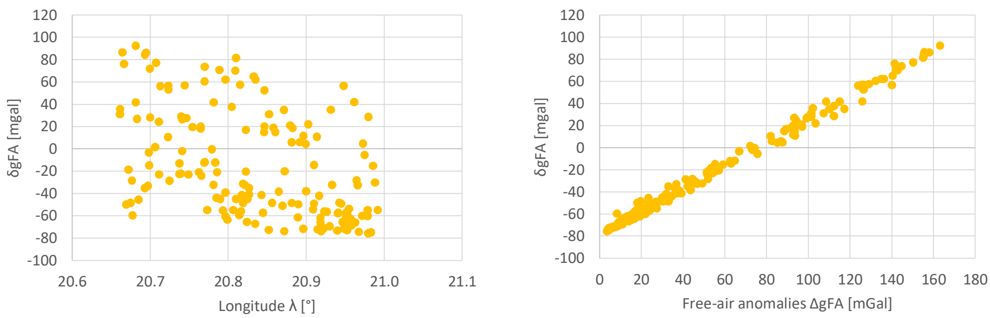

Figure 7. Gravity anomalies differences as a function of longitude (left) and free-air anomalies (right).

Figure 7 illustrates the differences as a function of longitude (left) and free-air anomalies (right). Similar to the latitude analysis, δg_{FA} show no dependence on longitude, with values ranging from −80 cm to 80 cm regardless of position. In contrast, the comparison with free-air anomalies reveals a clear trend consistent with the behavior observed against orthometric height. The differences start at approximately −80 mGal for free-air anomaly values near 0 mGal, decrease to about −10 to 10 mGal at 80 mGal, and increase again to around 80 mGal at free-air anomaly values of 160 mGal.

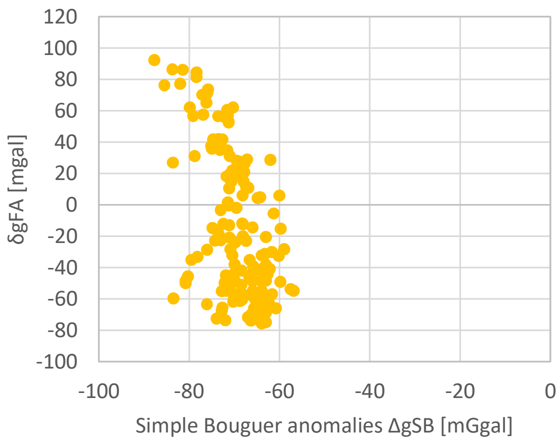

Figure 8. Gravity anomalies differences as a function of the simple Bouguer anomalies.

Figure 8 shows that the simple Bouguer anomalies range from −90 mGal to approximately 58 mGal. The differences in the free-air gravity anomalies, however, remain within −80 mGal to 80 mGal. Thus, no significant correlation is observed between the differences and the simple Bouguer anomalies.

3.3 Validation with varying maximum degree of expansion

The last validation method is done by using GGMs with varying maximum degree of expansion. The assessement process is done by using the δN from Eq. (10). In this process, N_{GGM} is computed for different $n_{\max} = 10, 30, 50, \dots, 240, 260, 280, 300$. For the differences in the geoid undulations, the mean and standard deviation are calculated.

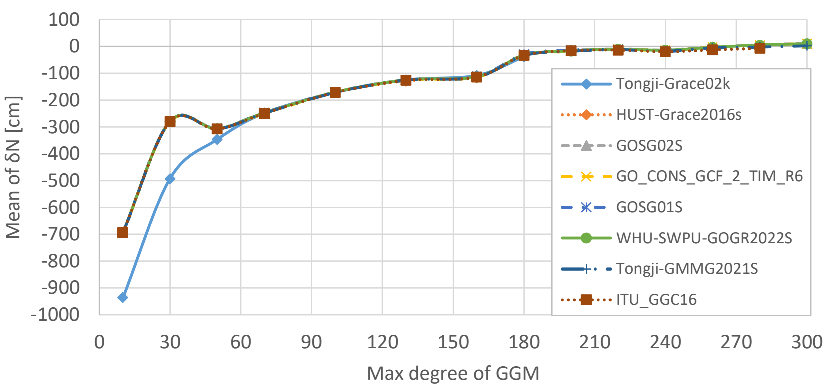

Figure 9. Statistics of the mean of the δN as a function of the maximum degree of expansion.

As shown in Figure 9, when comparing the δN for $10 < n_{\max} < 150$, the mean of δN ranges from -693 cm to -113 cm, indicating a decrease in the mean with increasing maximum degree. An exception is the Tongji-Grace02k model, which exhibits a mean of -935 cm for $n_{\max} = 10$, reaching values comparable to the other models for $n_{\max} = 70$. Beyond $n_{max} = 220$, all models converge to similar mean values. The minimum mean value of -2.78 cm is observed for the GOSG02S model at $n_{\max} = 260$.

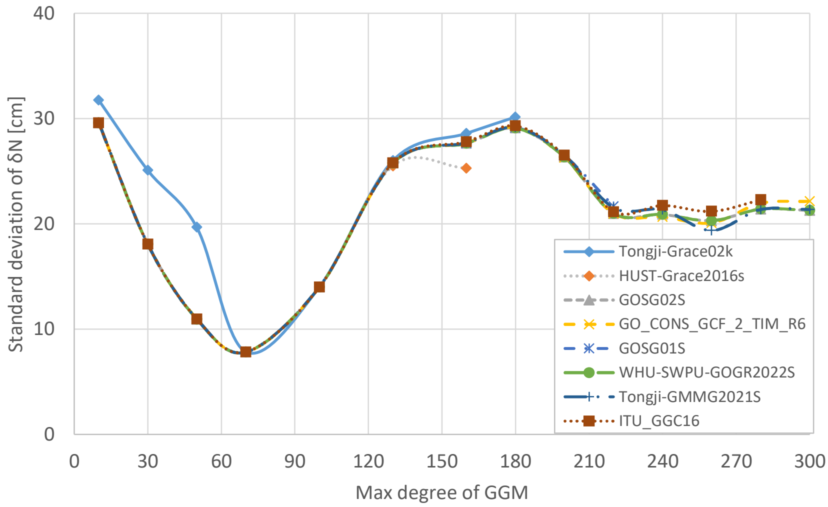

Figure 10. Statistics of the standard deviation of the δN as a function of the maximum degree of expansion

Figure 10 illustrates the relationship between the standard deviation of the δN and the maximum degree of expansion of the GGM. For $10 < n_{\max} < 70$, the standard deviation decreases from 30 cm to 8 cm. Subsequently, for $70 < n_{\max} < 180$, the standard deviation increases again, reaching approximately 28 cm. The trend declines up to $n_{\max} = 220$, when the values for standard deviation stabilizes around 21 cm. Beyond this, up to degree 300, the standard deviation fluctuates slightly between 20 cm and 22 cm.

4 CONCLUSION

This study provides a detailed evaluation of selected satellite-only GGMs over a region of complex topography in western Macedonia, utilizing both GNSS/leveling measurements and terrestrial gravity surveys. The assessments were conducted through three complementary methodologies: the comparison of geometric geoid undulations, the analysis of free-air gravity anomalies, and the investigation of geoid differences across varying maximum degrees of spherical harmonic expansion.

Comparison with GNSS/leveling data demonstrated that the majority of GGMs exhibited consistent performance, with RMS ranging from 21 cm to 22 cm. In contrast, the GRACE-only models (Tongji-Grace02k and HUST-Grace2016s) showed notably higher RMS values. Among the evaluated models, the GOCE-based GOSG02S model achieved the lowest RMS, indicating superior accuracy and stable performance throughout the study area. The analysis of δN as a function of orthometric height, geoid undulation, and gravity anomalies revealed a clear height-dependent trend, with larger discrepancies occurring in regions of higher elevation, while variations with latitude and geoid undulation remained minimal.

The validation on terrestrial gravity points exhibited similar trends. RMS values of δg_{FA} ranged between 44.65 mGal and 46.40 mGal, with the smallest differences observed for GOSG01S

(GOCE) and ITU_GGC16 (GOCE+GRACE). Differences generally increased with orthometric height and free-air anomalies, but showed little correlation with latitude, longitude, or simple Bouguer anomalies.

The analysis of geoid differences across varying maximum degrees of spherical harmonic expansion revealed that the mean δN decreases with increasing degree up to approximately $n_{\max} = 220$, beyond which all models converge toward comparable mean values. The standard deviation of δN exhibited an initial decline for low-degree expansions, followed by a subsequent increase and stabilization around 20–22 cm for $220 < n_{\max} < 300$.

Overall, the study demonstrates that modern satellite-only GGMs, particularly GOCE-based models, provide reliable representations of the Earth's long-wavelength gravity field over regions of complex topography. This study was conducted as a preliminary regional investigation. Future work may include the implementation of corrector surfaces to achieve potential vertical datum alignment, as well as a more detailed examination of the signal and error degree variances for the GGMs.

REFERENCES

Abbak, R. A., Sjöberg, L., Ellmann, A., Üstün, A. (2012). A precise gravimetric geoid model in a mountainous area with scarce gravity data: A case study in central Turkey. *Studia Geophysica et Geodaetica, 56*. https://doi.org/10.1007/s11200-011-9001-0

Akyilmaz O. Ustun A. Aydın C. Arslan N. Doganalp S. Guney C. Mercan H. Uygur S.O. Uz M. Yağcı O. 2016. High Resolution Gravity Field Determination and Monitoring of Regional Mass Variations using Low-Earth. Orbit Satellites Final Report of Project # 113Y155

AREC. (2025). Agency for Real Estate Cadastre of Republic of North Macedonia. https://www.katastar.gov.mk/en/home/

Brockmann, J. M., Schubert, T., Mayer-Gürr, T., Schuh, W.-D. (2019). The Earth's gravity field as seen by the GOCE satellite - an improved sixth release derived with the time-wise approach (GO_CONS_GCF_2_TIM_R6). *GFZ Data Services*. https://doi.org/10.5880/ICGEM.2019.003

Bruns, H. (1878). *Die Figure der Erde.* Berlin: Publ. Preuss.

Chen, J., Zhang, X., Chen, Q., Shen, Y., Nie, Y. (2022). Static Gravity Field Recovery and Accuracy Analysis Based on Reprocessed GOCE Level 1b Gravity Gradient Observations. *Paper presented at the EGU General Assembly 2022*. Vienna, Austria.

Chen, Q., Shen, Y., Francis, O., Chen, W., Zhang, X., Hsu, H. (2018). Tongji-Grace02s and Tongji-Grace02k: High-Precision Static GRACE-Only Global Earth's Gravity Field Models Derived by Refined Data Processing Strategies. *Journal of Geophysical Research: Solid Earth, 123(7)*, 6111-6137. https://doi.org/10.1029/2018JB015641

El-Ashquer, M., Al-Ajami, H., Zaki, A., Rabah, M. (2020). Study on the selection of optimal global geopotential models for geoid determination in Kuwait. *Survey Review, 52(373)*, 373-382. https://doi.org/10.1080/00396265.2019.1611256

Erol, B., Isik, M. S., Erol, S. (2020). An Assessment of the GOCE High-Level Processing Facility (HPF) Released Global Geopotential Models with Regional Test Results in Turkey. *Remote Sensing, 12*, 586. https://doi.org/10.3390/rs12030586

GFZ. (2025). Calculation of Gravity Field Functionals on Ellipsoidal Grids. https://icgem.gfz-potsdam.de/calcgrid

Godah, W., Krynski, J., Szelachowska, M. (2018). The use of absolute gravity data for the validation of Global Geopotential Models and for improving quasigeoid heights determined from satellite-only Global Geopotential Models. *Journal of Applied Geophysics, 152*, 38-47. https://doi.org/10.1016/j.jappgeo.2018.03.002

Heiskanen, A. W., Moritz, H. (1967). *Physical geodesy*. San Francisco and London: W. H. Freeman and Co.

Hofmann-Wellenhof, B., Mortiz, H. (2006). *Physical Geodesy*. Wien and NewYork: Springer.

Ince, E. S., Barthelmes, F., Reißland, S., Elger, K., Förste, C., Flechtner, F., Schuh, H. (2019). 15 years of successful collection and distribution of global gravitational models, associated services and future plans. *Earth System Science Data, 11(2),* 647-674. https://doi.org/10.5194/essd-11-647-2019

Kasapovski, F., Gospodinov, S., Srbinoski, Z., Dimov, L., Bogdanovski, Z., Gegovski, T. (2018). Vertical Crustal Movements in Seismic Active Regions. *Scientific Journal of Civil Engineering, 7(2).*

Moritz, H. (1980). Geodetic Reference System 1980. *Bull Geod, 54, 395-405*. https://doi.org/10.1007/BF02521480

Nyoka, C. J., Din, A. H. M., Pa'suya, M. F., Omar, A. H. (2022). Rigorous evaluation of global geopotential models for geoid modelling: A case study in Kenya. *Journal of African Earth Sciences, 194*, 104612. https://doi.org/10.1016/j.jafrearsci.2022.104612

Odalovic, O. (2009). *Study for the levelling and gravimetric network in R. of Macedonia*. Skopje: Agency for real estate cadastre of Macedonia.

Pham, H. T., Claessens, S., Kuhn, M., Awange, J. (2023). Performance evaluation of high/ultra-high-degree global geopotential models over Vietnam using GNSS/leveling data. *Geodesy and Geodynamics, 14(5)*, 500-512. https://doi.org/10.1016/j.geog.2023.03.002

Somigliana, C. (1929). Teoria generale del campo gravitazionale dell'ellissoide di rotazione. *Memorie della Società Astronomia Italiana, 4*.

Ustun, A., Abbak, R. A. (2010). On global and regional spectral evaluation of global geopotential models. *Journal of Geophysics and Engineering, 7(4)*, 369-379. https://doi.org/10.1088/1742-2132/7/4/003

Vaníček, P., Featherstone, W. E. (1998). Performance of three types of Stokes's kernel in the combined solution for the geoid. *Journal of Geodesy, 72(12),* 684-697. https://doi.org/10.1007/s001900050209

Varga, M. (2018). *The Application of Crustal Models in Regional Modelling of the Earth's Gravity Field* (doctoral thesis). Zagreb: Faculty of Geodesy, University of Zagreb. https://doi.org/10.13140/RG.2.2.11800.08963/2

Xu, X., Li, J., Zhao, Y., Wei, H. (2023). A GOCE only gravity model GOSG02S based on the SGG and SST observations. *GFZ Data Services*. https://doi.org/10.5880/icgem.2023.002

Xu, X., Zhao, Y., Reubelt, T., Tenzer, R. (2017). A GOCE only gravity model GOSG01S and the validation of GOCE related satellite gravity models. *Geodesy and Geodynamics, 8(4)*, 260-272. https://doi.org/10.1016/j.geog.2017.03.013

Yilmaz, N., Cakir, L. (2025). Contribution of the global geopotential models on gravimetric geoid determination: a case study of Colorado, USA. *Survey Review, 57*, 1-9. https://doi.org/10.1080/00396265.2025.2452795

Zhao, Yongqi; Li, Jiancheng; Xu, Xinyu; Su, Yong (2023). WHU-SWPU-GOGR2022S: A combined gravity model of GOCE and GRACE. GFZ Data Services. https://doi.org/10.5880/icgem.2023.003

Zhou, H., Luo, Z., Zhou, Z., Zhong, B., Hsu, H. (2017). HUST-Grace2016s: A new GRACE static gravity field model derived from a modified dynamic approach over a 13-year observation period. *Advances in Space Research, 60(3),* 597-611. https://doi.org/10.1016/j.asr.2017.04.026

Author:

Teaching assistant Filip Petrovski, MSc*
Faculty of Civil Engineering, Ss. Cyril and Methodius University – Skopje,
Str. „Partizanski Odredi“ nu. 24, 1000 Skopje, Republic of North Macedonia
E-mail: petrovski@gf.ukim.edu.mk

**Corresponding author / autor za korespodenciju*